
Finite Element Analysis of Tilting of Imitation Cat Paw Pad Tire

Mengyu Xie, Congzhen Liu^{*}, Chengwei Xu, Hui Meng, Aiqiang Li and Shicheng Lu

School of Transportation and Vehicle Engineering, Shandong University of Technology, China, Shandong, Zibo, Zhangdian, 255049.

^{*}Corresponding author email id: lcz200811@163.com

Date of publication (dd/mm/yyyy): 03/12/2020

Abstract – In this paper, a WALKWAY pressure distribution testing system and a 3D laser scanner were used to study the ground characteristics and topology of the cat paw pad, and the geometric shape of the cat paw pad was applied to the bionic structure design of 205/55R16 radial tire. The Hypermesh and ABAQUS software were used to build the model, and the accuracy of the model was verified by grounding test. The static load and brake simulation analysis of the tyre under tilting condition were carried out. The results show that under different tilting angles, compared with the sample tire, the bionic tire's ground area changes little, but the peak ground pressure and ground pressure skewness values are significantly reduced, which improves the distribution uniformity of ground pressure and helps to improve the partial wear of the tire. In addition, the grip of the bionic tire has also been improved. The bionic structure design alleviates the contradiction between the tire's grip and wear performance to a certain extent.

Keywords – The Bionic Tire, Tilting, Ground Pressure, Finite Element Analysis.

I. INTRODUCTION

Tire is an important part of automobile, which not only supports the body mass, transmits braking force, driving force and steering force to the ground, but also has an important influence on the ride comfort, handling and safety of automobile [1]. Under the condition of tilting, tire pressure distribution, ground area and other characteristics will change. Therefore, the grounding characteristics under the condition of tilting are of great significance to the vehicle handling stability and wear characteristics.

With the rapid development of modern science and technology, more and more high technology is applied to the design and improvement of tires. After many years of natural evolution, many animals have excellent geometric structures, unique material topologies, simple and effective control methods and functional surface structures. These structures, materials and the way of motion control make animals better than modern mechanical systems in terms of motion stability, flexibility, robustness and environmental adaptability [2]. Lidong Liu [3] introduced the tread pattern of a motorcycle modeled on the “antler shape”, which improved the drainage, grip and wear resistance of the tire. Guolin Wang [4] designed the structure of tire crown in imitation of locust foot meridian tire, and improved the ground grasping and wear performance of the tire. The polymer Research Center in Madison, Wisconsin, USA, USES the bionic principle to support the honeycomb hexagon structure to each other for the tire design, thus achieving the effect of reducing vibration, improving wheel strength and avoiding tire puncture [5]. Haichao Zhou [6] introduced a non-smooth structure of micro-circumferential grooves on the skin surface of shark, and applied it to the design of tires, which effectively reduced the dynamic tread pressure of tires when driving on water film and improved the anti-skid performance of tires. In order to increase the vehicle's passability in the desert, Jie Li et al. studied the imitation camel's foot tire and developed the test tire [7]. The imitation panther's claw tire developed by German Continental company improves the ground grip of the tire and reduces the rolling resistance [8]. Likun Zhou et al. [9] designed the copycat fish sucker type ice anti-skid tire, which improved the anti-skid performance of the tire on the ice and

snow road. It can be seen from these studies at home and abroad that bionic technology has a good effect in the research of improving tire performance.

WALKWAY pressure distribution testing system and 3D laser scanner were used to study the ground characteristics and topology of cat paw pad, and the geometric shape of cat paw pad was applied to the bionic structure design of 205/55R16 radial tire. Finite element software is used to analyze the static load and rolling ground characteristics of tire under tilting condition in order to improve the ground performance of tire.

II. IMITATION CAT PAW PAD TIRE SHOULDER STRUCTURE DESIGN

After millions of years of natural evolution, the cat has become an advanced environmental adaptor in nature. Its PAWS have reliable grip and buffering performance, which ensures the excellent sports ability of the cat [10]. The WALKWAY pressure distribution test system and OLYMPUS high speed camera were used to obtain the ground characteristics of cat paws, Fig. 1 shows the peak vertical force of the fore and hind paws at different speeds. The vertical forces were normalized to the individual cat's body weight and expressed as % BW. It can be seen from the figure that the peak vertical force of the cat's fore paw is significantly greater than that of the hind paw. It indicates that the fore paw plays a major role in supporting and controlling direction when cats are in motion [11]. Therefore, the forepaw is selected as the research object.

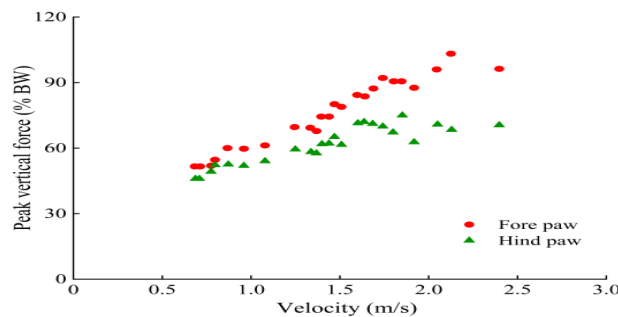


Fig. 1. Peak vertical force of cat fore and hind paws at different speeds.

The vertical reaction between the paw pad of the cat's front paw and each paw toe was extracted, and the ground pressure variation curve of each part was drawn, as shown in Fig. 2. It can be seen from the figure that during the stable contact between the cat's front paws and the ground, the paw pad is always the place with the greatest stress. The variation trend of the ground reaction at other velocities is consistent. This indicates that when the cat's front paw is grounded, the palm pad is the main supporting force. Taking this as inspiration, the contour features of cat front paw pad were extracted and applied to the design of shoulder arc of passenger car tires.

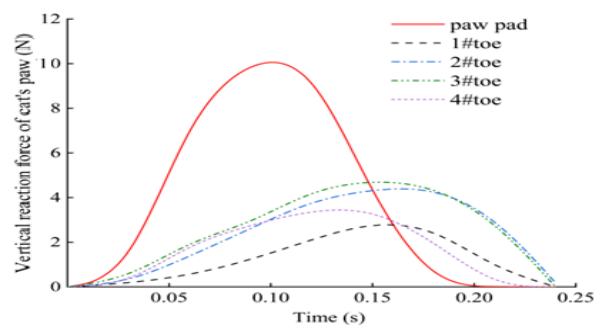


Fig. 2. The reaction curve of each part of cat's front paw.

VIVID 910 3D laser scanner is used to scan the paw pad of the cat, and the precise geometric figure of the paw is obtained. The software IMAGEWARE was used to simplify the geometric figure, as shown in Fig. 3. Cross-section points were selected for curve fitting to obtain the cross-section curve of the paw pad of cat, as shown in Fig. 4.

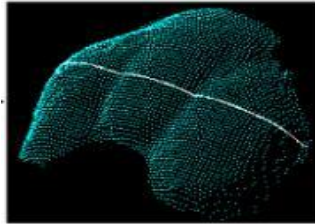


Fig. 3. Cat claw point cloud processing result diagram.

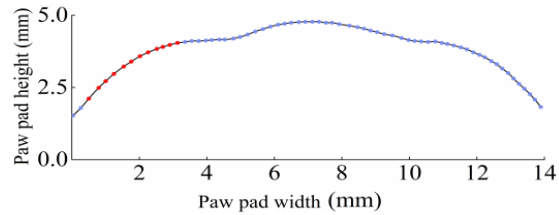


Fig. 4. Cat paw pad point cloud cross-section fitting curve.

On the basis of the point cloud at the shoulder of the palm cushion section (Fig. 5 red curve), polynomial fitting was performed, where the fitting equation was:

$$y = 1.4439 + 1.5510x - 0.2709x^2 + 0.0131x^3 \quad (1)$$

According to the “similarity principle” [12] and taking equation (1) as the prototype, the shoulder arc of the tire was bionic designed. As shown in Fig. 5, the shoulder arc of the bionic tire is marked in red in the figure.

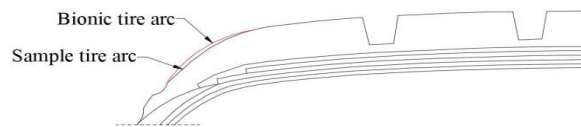


Fig. 5. 205/55 R16 tire shoulder arc.

III. FINITE ELEMENT MODEL OF TIRE

A. Material Model

The finite element model of 205/55R16 radial tire was established by Abaqus software. Because the tire structure is complex and the rubber material is nonlinear, different materials are used to characterize each part of the tire. The rubber part is simulated by CGAX3H and CGAX4H units. The tire body and belt layer are rubber-cord composite materials, which are simulated by Rebar material model. The properties of Rebar material model are shown in Table 1. Yeoh material model is adopted to simulate rubber materials such as tread and tread. The constitutive equation of strain energy of Yeoh model is as follows [13]:

$$W = C_{10}(I_1 - 3) + C_{20}(I_1 - 3)^2 + C_{30}(I_1 - 3)^3 \quad (2)$$

Where W is the strain energy; C_{10} , C_{20} , and C_{30} are the expansion coefficients of the third-order reduced polynomial; I_1 is the first invariant of strain.

Table 1. Reinforcement material properties.

Rebar material	Young's modulus (MPa)	Poisson's ratio (μ)	Density (kg/m ³)	Cord Angle (°)
Belt steel wire 1	105900	0.29	7800	66
Belt steel wire 2	105900	0.29	7800	114

Rebar material	Young's modulus (MPa)	Poisson's ratio (μ)	Density (kg/m ³)	Cord Angle (°)
Carcass cords	5250	0.3	1350	0

B. Load and Boundary Conditions

The motion state of the tire includes the translational and circumferential rotation of the forward direction. During the simulation of the tire, the rolling of the tire on the road was simulated by controlling the moving speed and circumferential rotation speed of the tire [14]. A set of contact points is defined on the periphery of the tire rim. The edges of the mesh between the points are defined as rigid body line units, which act as the rim of the tire. The action of the rim is simulated by applying constraints on the set of points. Apply upward concentrated force to the road surface to simulate tire loading, on the basis of static load, the tire brake is simulated by controlling the moving speed and rotating speed of the tire. The tyre tilt condition is simulated by tilting the road surface. The load applied to the tire during static loading is 4000N. Fig. 6 shows the section model and three-dimensional finite element model of the tire.

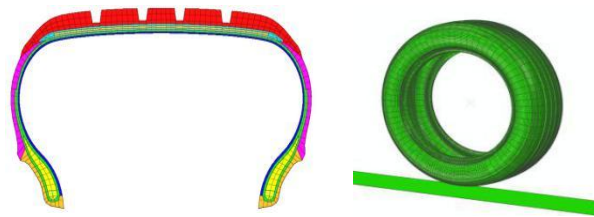


Fig. 6. Finite element model of tire.

C. Model Validation

In order to verify the reliability of the model, static loading test is carried out on the tested tire. The maximum rated load of the tire is 6150N and the charging pressure is 2.6bar. The comparison between the load-subsidence curve test and simulation results under static loading is shown in Fig. 7. The relationship between load and subsidence is approximately linear, and the error between test and simulation is very small.

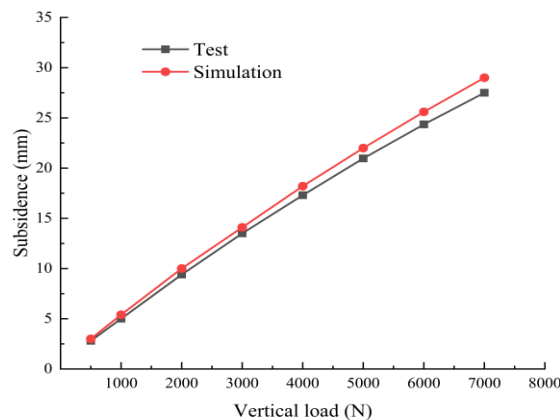


Fig. 7. Load - subsidence curve.

The shape of the ground imprint obtained by test and simulation is compared, as shown in Fig. 8. The shape and distribution of ground imprinting obtained by experiment and simulation have good consistency. The comparison between the experimental and simulated ground imprinting values is shown in Table 2, and the maximum error is 4.0%. It can be seen that the simulation results have a good consistency, which indicates that

the finite element model of the tire is highly accurate.

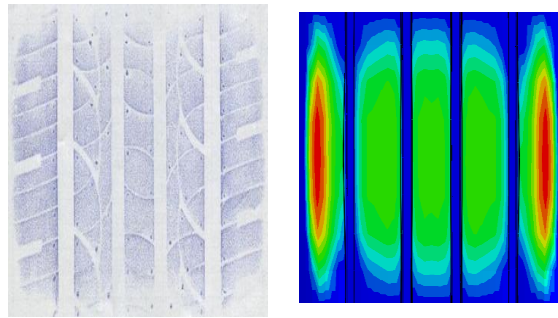


Fig. 8. Contact patch shape under static load.

Table 2. Comparison of contact patch test and simulation results.

Project	Test	Simulation	Relative error /%
Long axis length of contact patch /mm	128.45	132.19	2.9
short axis length of contact patch /mm	101.20	103.64	2.4
Grounding area /mm ²	13000	13700	5.3

IV. RESULTS AND DISCUSSION

In order to compare the roll grounding characteristics of the sample tire and the bionic tire, the static load and brake grounding performance of the tire were studied under the conditions of an air pressure of 2.6bar and a load of 4000N with a tilt Angle of 2°, 4°, 6° and 8°.

The uniform distribution of ground pressure was used to investigate the change of tire wear performance. The skewness value of ground pressure is an index to describe the uniform distribution of ground pressure in the ground connection of a tire. The smaller the skewness value of ground pressure is, the better the uniform distribution of ground pressure is [15]. Its calculation formula is as follows:

$$\alpha = \sqrt{\frac{1}{n-1} \sum (p_i - \bar{p})^2} \tag{3}$$

Where: n is the number of nodes in the earthing imprinting, p_i is the pressure value of the first i point in the earthing imprinting, and \bar{p} is the average value of the distributed pressure in the whole earthing imprinting.

A. Static Load Grounding Performance Analysis

According to the lateral static loading analysis, the ground pressure distribution of the sample tire and the bionic tire under different tilting angles was obtained, as shown in Fig. 9. Table 3 shows the tilting ground data of tire under static load. It can be seen from Figure 10 and Table 3 that, The variation trend of the ground imprinting of the sample tire and the bionic tire is similar and decreases with the increase of the lateral inclination. On the ground side, the imprinted length will increase, while on the other side, it will decrease and gradually change from trapezoid to triangle. Under different tilting angles, compared with the sample tire, the ground area of the bionic tire did not change significantly, but both the peak ground pressure and the skewness of the ground pressure decreased significantly, the high ground pressure area of the tire shoulder increased, and

the stress concentration area decreased. The results show that the bionic structure design is helpful to improve the uniformity of ground pressure distribution and enhance the tire wear performance under static load tilting condition.

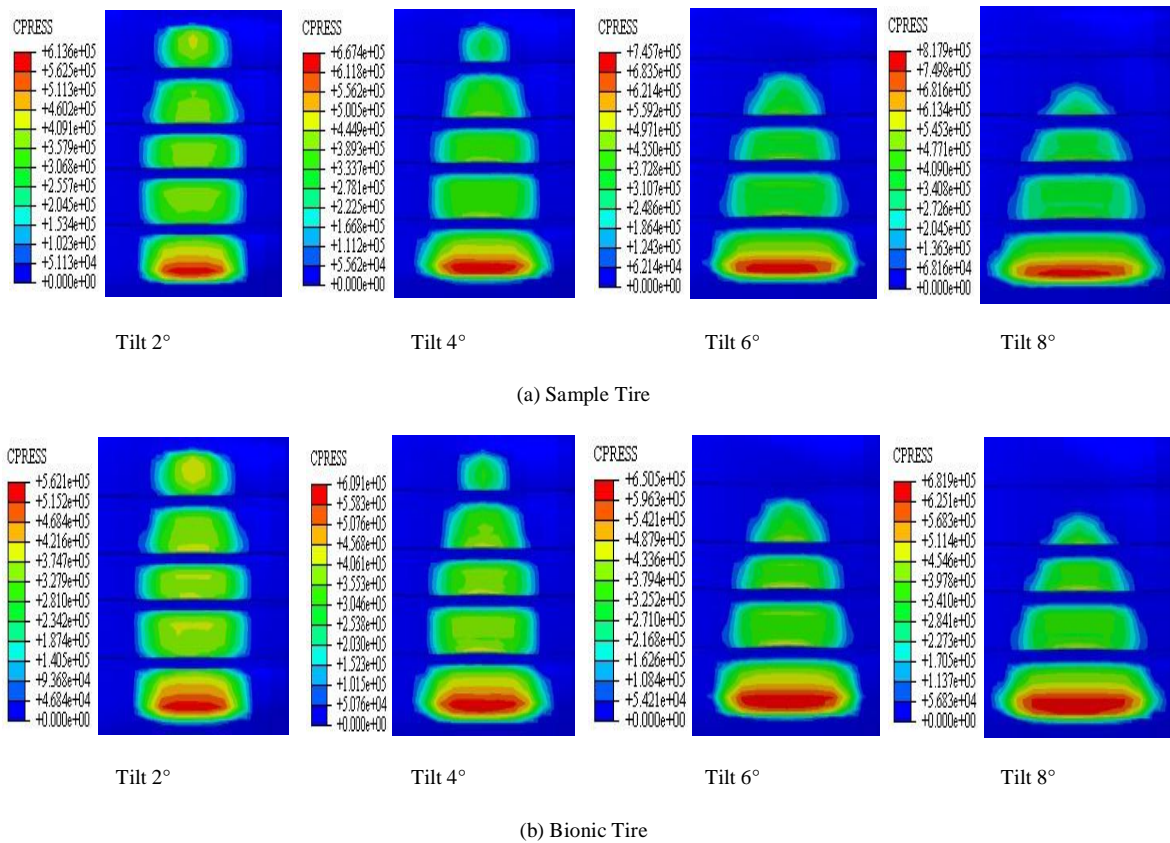


Fig. 9. Distribution of static load ground pressure under different tilt angle.

Table 3. Tyre tilting ground data under static load.

Scheme	Peak Ground Pressure/MPa			Ground Pressure Deflection Value/MPa			Ground Contact Area/cm ²		
	Sample Tire	Bionic Tire	Difference Value	Sample Tire	Bionic Tire	Difference Value	Sample Tire	Bionic Tire	Difference Value
2°	0.6136	0.5621	-8.4%	0.1432	0.1356	-5.3%	141.91	142.75	0.59%
4°	0.6674	0.6091	-8.7%	0.1512	0.1395	-7.7%	137.97	139.75	1.29%
6°	0.7457	0.6505	-12.8%	0.1685	0.1536	-8.8%	130.81	133.21	1.83%
8°	0.8179	0.6819	-16.6%	0.1816	0.1648	-9.3%	128.31	130.47	0.89%

B. Brake Grounding Performance Analysis

In the process of tire driving and braking, the ground simulation analysis is only carried out in the process of tire braking because of the same action mechanism of road surface on tire force. Fig. 10 shows the distribution of tyre brake tilting ground pressure. It can be seen from the figure that, in the braking state, the ground pressure distribution is no longer symmetrical about the short axis of the ground, and the ground pressure at the front end of the brake becomes larger.

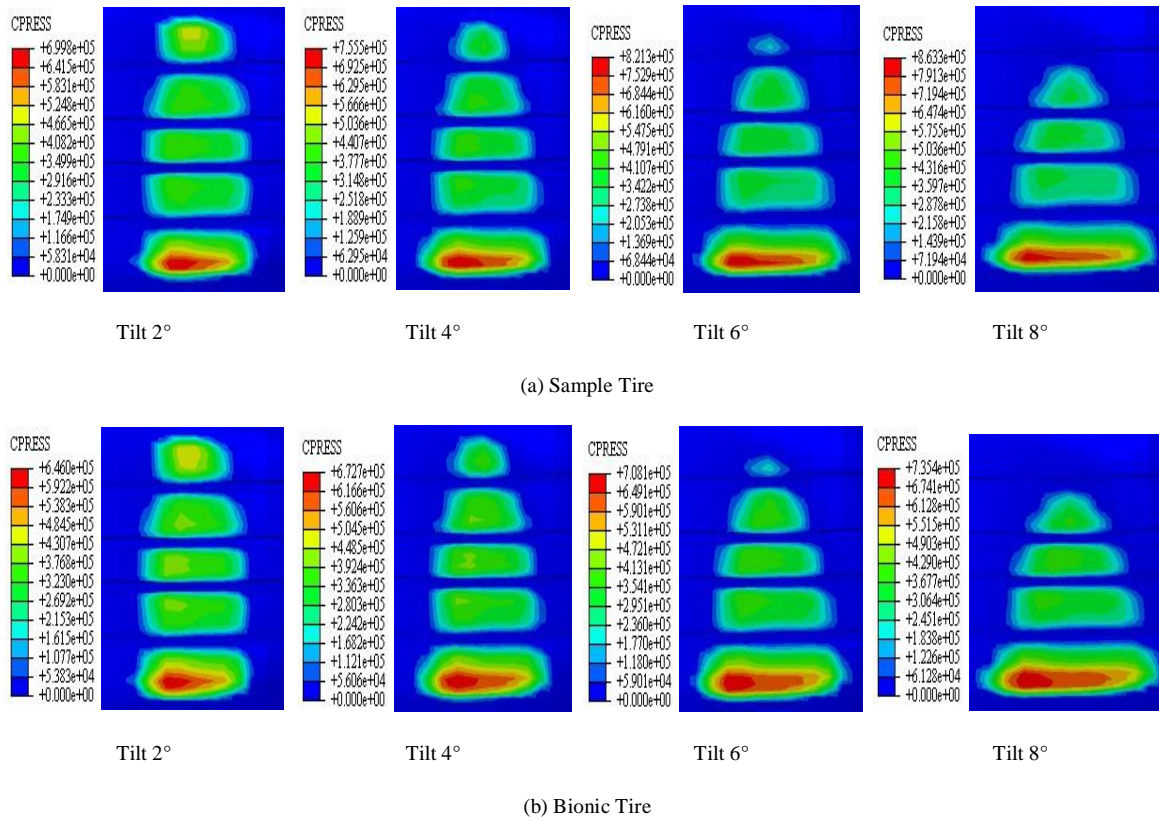


Fig. 10. Distribution of tire brake ground pressure under different tilt angle.

Table 4 shows the tyre brake tilt ground data. It can be seen from Table 4 that the peak ground pressure and ground pressure skewness value of the sample tire and the bionic tire both increase with the increase of the tilt angle. The increase of the peak ground pressure and the skewness of the ground pressure will make the ground pressure distribution more uneven, increase the stress concentration of the tire shoulder and aggravate the wear of the tire shoulder. Compared with the two kinds of tires, the peak ground pressure of the bionic tire is reduced to a maximum of 14.6%, and the skewness of the ground pressure is reduced to a maximum of 6.9%. This shows that the bionic structure design can reduce the uneven distribution of ground pressure and help to improve the wear performance of tire shoulder position.

Table 4. Tyre brake tilting ground data.

Scheme	Peak Ground Pressure/MPa			Ground Pressure Deflection Value/MPa			Ground Contact Area/cm ²		
	Sample Tire	Bionic Tire	Difference Value	Sample Tire	Bionic Tire	Difference Value	Sample Tire	Bionic Tire	Difference Value
2°	0.6998	0.6460	-7.7%	0.1472	0.1402	-4.8%	149.25	150.58	0.89%
4°	0.7555	0.6727	-11.0%	0.1579	0.1490	-5.6%	147.52	149.71	1.48%
6°	0.8211	0.7081	-13.8%	0.1824	0.1699	-6.9%	145.88	146.76	0.60%
8°	0.8611	0.7355	-14.6%	0.1918	0.1801	-6.1%	136.38	137.05	0.49%

Fig. 11 shows the grip curve of tire braking under different tilt angle. As can be seen from the figure, with the increase of the tilt angle, the tire grip presents a downward trend. The grip of the bionic tire is greater than that

of the sample tire, because the ground pressure distribution of the bionic tire shoulder is more even, and the area of the high pressure area of the tire shoulder is increased, thus improving the ground grasping performance of the tire to a certain extent. To sum up, under the premise of improved grip, the tire shoulder partial wear was greatly improved, and the bionic structure design alleviated the contradiction between the tire's grip and wear performance.

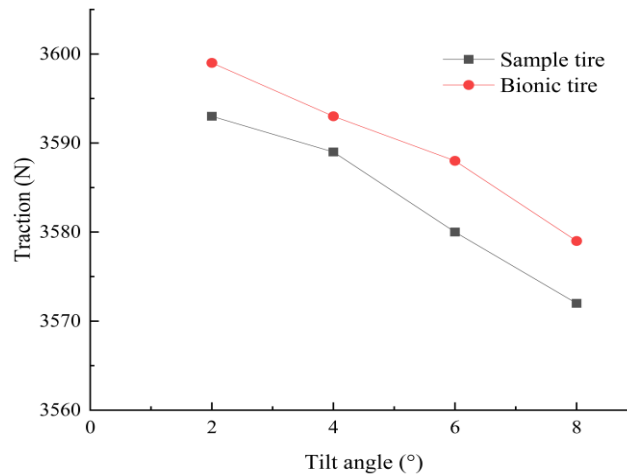


Fig. 11. Curve of tire brake grip under different tilt angle.

V. CONCLUSION

The structural characteristics of the cat's paw were studied. The geometric shape of the cat's paw was obtained by the scanner. Based on the geometric shape of the cat's paw pad, the tire shoulder structure of 205/55R16 radial tire was designed. The finite element software was used to build the model and carry out simulation analysis, and the following conclusions were drawn:

1. Under the tilting static load condition, the change of ground imprinting of the sample and bionic tire decreases with the increase of the lateral inclination and gradually changes from trapezoid to triangle. Compared with the sample tire, the peak ground pressure and ground pressure skewness of the bionic tire decreased significantly, and the stress concentration area of the tire shoulder decreased. The results show that the design of bionic structure is helpful to improve the distribution uniformity of ground pressure under tilting static load.
2. Under the tilting braking condition, the ground pressure distribution is shifted and the ground pressure at the front end of the braking becomes larger. The value of peak ground pressure and ground pressure skewness of the sample tire and the bionic tire increased with the increase of lateral inclination. Compared with the sample tire, the peak ground pressure of the bionic tire was reduced by 14.6% at most, and the skewness of ground pressure was reduced by 6.9% at most, and the grip of the bionic tire was greater than that of the sample tire. It shows that the bionic structure design alleviates the contradiction between the tire's ground grasping and wear performance to some extent.

REFERENCES

- [1] Shou-bin Yang, Chang-dong Shu, Yong-ping Shu. Finite element Analysis of roll ground performance of tire with complex pattern. Rubber industry, 2012, 59(12): 740-743.
- [2] Dickioson M.H., Farley C.T., Full R.J., et al. How animals move: An integrative view. Science, 2000, 288(7): 100-106.
- [3] Li-dong Liu. The latest model of motorcycle tires. Motorcycle Technology, 1991(4): 42.

- [4] Guo-Lin Wang, Yin-Wei Ma, Chen Ling, et al. Structure design of radial tire crown imitating locust foot. Journal of mechanical engineering, 2013, 49(12): 131-135.
- [5] Bo Su. Cooper Bionic Honeycomb Tire. Rubber Technology Market, 2009(10): 14.
- [6] Hai-chao Zhou, Guo-lin Wang, Yang-min Ding, Jian Yang, Hui-hui Zhai, Hoon Eui Jeong. Investigation of the Effect of Dimple Bionic Non-smooth Surface on Tire Antihydroplaning. Applied Bionics and Biomechanics, 2015, 2015.
- [7] Jie Li, Ji-de Zhuang, Dong Wei. Design and Experimental study of imitation camel's foot rubber used in desert. Journal of agricultural engineering, 1999, 15(2):32-36.
- [8] Ke-shu Ye. New progress of tire technology in the world. Rubber Technology and Equipment, 2001(3): 1-11.
- [9] Li-kun Zhou, Hong-wei Wang. Tread pattern design and finite element analysis of copycat fish sucker. Journal of xi 'an university of technology, 2013, 29(2): 228-231.
- [10] Xiao-peng Zhang, Jia-ling Yang, Hui Yu. Analysis of the Cushioning mechanical properties of feline foot pads. Journal of Biomedical Engineering, 2012, 029(006): 1098-1104.
- [11] Ya-zhong Liu. Research on gait Planning and Control Method of Crawling Motion of feline quadruped Robot. Harbin university of Science and Technology, 2018.
- [12] Huan-huan Zuo. Application exploration of similarity principle. Industry and technology forum, 2016, 15(20): 73.
- [13] Jun Wang, Liang Li, Lin Sun. Finite element analysis of 245/70R16 tires. Tire Industry, 2016, (9): 520-528.
- [14] Zhao Li, Jie-ran Li, Yuan-ming Xia. Experimental study and numerical analysis of tire contact friction behavior. Journal of Shanghai jiaotong university, 2013, 47(5): 13-18.
- [15] Chen Liang. Research on the Comprehensive grounding performance Evaluation System and Method of radial tire. Zhenjiang: Jiangsu University, 2013.

AUTHOR'S PROFILE



First Author

Mengyu Xie, Master in reading, Male, School of Transportation and Vehicle Engineering, Shandong University of Technology, China, Shandong, Zibo, Zhangdian, 255049. email id: 328097596@qq.com.



Second Author

Congzhen Liu*, Doctor of Engineering, Male, Associate professor. School of Transportation and Vehicle Engineering, Shandong University of Technology, China, Shandong, Zibo, Zhangdian, 255049 (Correspondence author).



Third Author

Chengwei Xu, Master in reading, Male, School of Transportation and Vehicle Engineering, Shandong University of Technology, China, Shandong, Zibo, Zhangdian, 255049.



Fourth Author

Meng Hui, Master in reading, Male, School of Transportation and Vehicle Engineering, Shandong University of Technology, China, Shandong, Zibo, Zhangdian, 255049.



Fifth Author

Ai qiang Li, Master in reading, Male, School of Transportation and Vehicle Engineering, Shandong University of Technology, China, Shandong, Zibo, Zhangdian, 255049.



Sixth Author

Shicheng Lu, Master in reading, Male, School of Transportation and Vehicle Engineering, Shandong University of Technology, China, Shandong, Zibo, Zhangdian, 255049.